EBioMedicine 42 (2019) 174–187

Contents lists available at ScienceDirect

EBioMedicine

journal homepage: www.ebiomedicine.com

EBioMedicine
Published by THE LANCET

Toxic amyloid-β oligomers induced self-replication in astrocytes triggering neuronal injury

Wei Wang [a,b], Ting-ting Hou [a], Long-fei Jia [a,b,c], Qiao-qi Wu [a,b,c], Mei-na Quan [a], Jian-ping Jia [a,b,c,d,e,f,*]

[a] Inovation Center for Neurological Disorders, Department of Neurology, Xuan Wu Hospital, Capital Medical University, Beijing 100053, PR China
[b] Beijing Key Laboratory of Geriatric Cognitive Disorders, Beijing 100053, PR China
[c] Clinical Center for Neurodegenerative Disease and Memory Impairment, Capital Medical University, Beijing 100053, PR China
[d] Key Laboratory of Neurodegenerative Diseases, Ministry of Education, Beijing 100053, PR China
[e] National Clinical Research Center for Geriatric Disorders, Beijing 100053, PR China
[f] Center of Alzheimer's Disease, Beijing Institute for Brain Disorders, Beijing 100053, PR China

ARTICLE INFO

Article history:
Received 18 November 2018
Received in revised form 3 March 2019
Accepted 18 March 2019
Available online 27 March 2019

Keywords:
Alzheimer's disease
PS1V97L transgenic mice
Amyloid-β oligomers
Astrocyte
BACE1
Apolipoprotein E

ABSTRACT

Background: Soluble amyloid-β oligomer (AβO) induced deleterious cascades have recently been considered to be the initiating pathologic agents of Alzheimer's disease (AD). However, little is known about the neurotoxicity and production of different AβOs. Understanding the production and spread of toxic AβOs within the brain is important to improving understanding of AD pathogenesis and treatment.
Methods: Here, PS1V97L transgenic mice, a useful tool for studying the role of AβOs in AD, were used to identify the specific AβO assembly that contributes to neuronal injury and cognitive deficits. Then, we investigated the production and spread of toxic Aβ assemblies in astrocyte and neuron cultures, and further tested the results following intracerebroventricular injection of AβOs in animal model.
Findings: The results showed that cognitive deficits were mainly caused by the accumulation of nonameric and dodecameric Aβ assemblies in the brains. In addition, we found that the toxic AβOs were duplicated in a time-dependent manner when BACE1 and apolipoprotein E were overexpressed, which were responsible for producing redundant Aβ and forming nonameric and dodecameric assemblies in astrocytes, but not in neurons.
Interpretation: Our results suggest that astrocytes may play a central role in the progression of AD by duplicating and spreading toxic AβOs, thus triggering neuronal injury.
Fund: This study was supported by the Key Project of the National Natural Science Foundation of China; the National Key Scientific Instrument and Equipment Development Project; Beijing Scholars Program, and Beijing Brain Initiative from Beijing Municipal Science & Technology Commission.

1. Introduction

Alzheimer's disease (AD) is a neurodegenerative disorder associated with progressive neuronal death and memory loss [1]. According to the amyloid cascade hypothesis, amyloid-β (Aβ) fiber have been recognized as the initiating pathologic agents in AD [2]. However, because the extent of insoluble, deposited amyloid is poorly correlated with cognitive impairment, research efforts have focused on soluble forms of Aβ, also referred to as Aβ oligomers (AβOs) [3,4]. Mounting evidence has been accumulated over the last 15 to 20 years, indicates that soluble AβOs, rather than insoluble fibrilsor plaques, trigger synapse failure and memory impairment [5–8]. Soluble AβOs have therefore received a great deal of attention in the analysis of AD pathogenesis. Subsequent studies have substantiated the notion that Aβ assembly pathways lead to AβOs with different molecular masses. However, which forms of AβOs are responsible for instigating AD neuronal damageremains an unresolved issue.

What is known about the cellular mechanisms underlying the production and spread of AβOs remains very limited , despite decades of research focused on neuronal abnormalities. However, one of the earliest neuropathological changes observed in AD is the accumulation of reactive astrogliosis at sites of Aβ deposition [9–11], and Aβ-associated tissue damage is correlated with both the amount of Aβ and the extent of reactive astrogliosis [12,13]. Astrogliosis is the process by which astrocytes respond to insult or injury in the central nervous system (CNS), and encompasses a spectrum of molecular and morphological

* Corresponding author at: 45# Changchun Street, Xicheng District, Beijing 100053, PR China.
E-mail addresses: jiajp@vip.126.com, jjp@ccmu.edu.cn (J. Jia).

https://doi.org/10.1016/j.ebiom.2019.03.049

Research in context

Evidence before this study

The soluble amyloid-β oligomers (AβOs) are recently considered to be the initiating pathologic agents of Alzheimer's disease (AD). However, little is known about the neurotoxicity and production of AβOs.

Added value of this study

We found that the toxic AβOs were nonameric and dodecameric Aβ assemblies, which could induce self-replication by increasing the expression of BACE1 and apoE in astrocytes but not neurons.

Implications of all the available evidence

Our study demonstrated that the specific Aβ assemblies instigating cognitive deficits were nonamer and dodecamer, which offered the potential for developing precise diagnostic biomarker to detect their correlate in humans with preclinical AD. We also revealed that the toxic AβOs were produced and spreaded mainly in astrocytes by inducing the over-expression of apoE, suggesting a novel mechanism underlying apoE function in progression of AD, which opened a new perspective to search for therapeutic targets for AD.

changes [14,15]. A number of studies have shown that reactive astrogliosis has the potential to contribute to CNS disease mechanisms through either the loss of normal functions or the gain of detrimental effects [16]. Consistent with the notion that astroglial cells play a role in AD, astrocyte activation is triggered by the infusion of AβOs in the brain [9,17]. It is therefore conceivable that there is some connection between the production and spread of AβOs and astrocytes.

PS1V97 L transgenic (PS1V97L-Tg) mice express a human *PSEN1* variant linked to AD that was first reported a single missense mutation Val97Leu (V97 L) of *PSEN1* in a Chinese pedigree suffering from early onset AD in our previous study [18–21]. This model supports the notion that AβOs play an initial role in the onset of AD and provides a useful tool for studying the role of AβOs in AD pathogenesis. We also found that activated astrocytes were more evident during the emergence of AβOs in the cerebral cortex and hippocampus in PS1V97L-Tg mice [18]. In this study, we investigated the pathogenicity of various Aβ species in PS1V97L-Tg mice and explored the roles of astrocytes and neurons in the production and spread of Aβ assemblies.

2. Materials and methods

2.1. Animals and cells

PS1V97L-Tg mice aged 6–24 months old were housed in a room at constant temperature (25 ± 1 °C) and humidity (40%–60%) with a 12 h light/dark cycle (lights on at 8:00 AM). The animals had free access to food and water. PS1V97L-Tg mice expressing the human PSEN1 gene with the V97 L mutation were generated as previously described. The PS1V97LTg mouse lines were maintained by crossing heterozygous transgenic mice with wild-type C57BL/6 animals. Mice were screened by polymerase chain reaction (PCR) to determine their genotypes, as previously described (Wang et al., 2012). ApoE$^{-/-}$ mice with a C57BL/6 background and Sprague-Dawley rats were obtained from the Vital River Laboratory (China) and raised in Xuanwu Hospital Animal House.

2.2. Antibodies and reagents

Antibodies to the following targets were used: mouse monoclonal anti-Aβ (4G8) (BioLegend, Cat#800701, RRID:AB_2564633), chinken polyclonal anti-GFAP (Millipore, Cat# AB5541, RRID:AB_177521), mouse monoclonal anti-GFAP (Millipore, Cat# MAB360, RRID:AB_11212597), rabbit polyclonal anti-BACE1 (abcam, Cat# ab2077, RRID:AB_302817), rabbit polyclonal anti-sAPPβ (BioLegend, Cat# 813401, RRID:AB_2564769), rabbit monoclonal anti-MAP2 (abcam, Cat# ab96378, RRID:AB_10678243), rabbit monoclonal anti-β-actin (Santa Cruz Biotechnology, Cat# sc-47778, RRID:AB_2714189), rabbit monoclonal APOE antibody (Invitrogen, Cat# 701241, RRID:AB_2532438), mouse monoclonal anti-Aβ (6E10) (BioLegend, Cat# 805701, RRID:AB_2564982), rabbit polyclonal anti-A11 (Thermo Fisher, Cat# AHB0052, RRID:AB_1501357), apolipoprotein E2/3/4 human (PEPROTECH), human Beta-Amyloid [1–42] (Thermo Fisher), LY2886721 (Selleck), Amyloid-beta 42 Rat/Mouse ELISA Kit (IBL), Amyloid-beta 40 Rat/Mouse ELISA Kit (IBL), Pierce™ Direct IP Kit (Thermo Fisher), Cytotoxicity Detection kit (Roche). DMEM/F-12 (Thermo Fisher), Neurobasal™ medium (Thermo Fisher), fetal bovine serum (Thermo Fisher), B-27™ Supplement (Thermo Fisher). All chemicals not listed above were purchased from Sigma-Aldrich.

2.3. Behavioral tests

The animals were tested for spatial learning and memory in a Morris water maze (MWM) to assess age-dependent cognitive impairments. The animal were kept under a 12 h:12 h light-dark cycle to ensure that the tests were carried out during the animals' active period. For 5 consecutive days, all animals were trained to find a platform hidden below the water surface in a circular tank (diameter, rats: 180 cm; mice: 150 cm). The MWM protocols were carried out by coworkers who were blinded to the genotypes. Training consisted of four trials per day performed at a 60-s intertrial interval. If the animals failed to find the escape platform within 120 s (rats) or 60 s (mice) by themselves, they were placed on the platform for 10 s by the experimenter. After the animal climbed onto the platform, it was allowed to remain there for 10 s before the commencement of the next trial. On the sixth day, trained spatial memory was assessed using a probe trial, which included a 60-s free search of the pool without the platform. The time spent in the target quadrant, where the platform had been located, was recorded with a DNS-2 type MWM testing set equipped with an online video tracking system (camera, TOTA-450III, Japan).

2.4. Intracerebroventricular (i.c.v.) injection of AβOs

Sprague-Dawley male rats and apoE$^{-/-}$ male mice (approximately 3 months old (young adults)), were used to test the effects of natural AβO infusions on memory. The animals were anesthetized with isoflurane inhalation at an induced concentrationof 2–2.5%.Then, the animals were placed in a stereotaxic apparatus, and isoflurane at a maintained concentration of 1–1.5%was administered to maintain anesthesia. After disinfecting the skin with alcohol, the scalp was shaved to expose the skull, and cannulae were implanted into a lateral ventricle (rat coordinates for the cannula tip, from bregma: ML = 1.5 mm; AP = 1 mm; DV = 3.5 mm; mouse coordinates for the cannula tip, from bregma: ML = 1 mm; AP = 0.5 mm; DV = 2.4 mm). A 10 μM solution of AβO or elution buffer for immunoprecipitation was applied at a volume of 6 μL (rats) and 2 μL (mice),which was injected gradually (1 μL/min) once every other day for a total ofthree times. Behavioral tests were performed 20 and 40 days after the first injection.

2.5. Protein extractions

Ice-cold Tris-buffered saline (TBS)consisting of 20 mM Tris-HCl, 150 mM NaCl (pH 7.4), 1% Triton X-100, 2% SDS, 1 mM

phenylmethylsulfonyl fluoride (PMSF), and a protease inhibitor cocktail (Roche) was added to the frozen hemisphere (excluding the cerebellum),which was then homogenized using a mechanical Dounce homogenizer and then centrifuged for 30 min at 13,000*g*. The extracts were frozen within 1–2 min of collection and stored at −80 °C.

2.5.1. Immunoprecipitation of Aβ oligomers

Aβ oligomers were purified with a Thermo Scientific™ direct immunoprecipitation Kit (Thermo Scientific) according to the manufacturer's instructions. Couple 4G8 Antibody to AminoLink Plus Coupling Resin. One to two milligrams of total brain proteins obtained from PS1V97 L mice was added to the antibody-coupled resin in the spin column, which was then incubated while shaking for 1 h at room temperature and then overnight at 4 °C. Immunocaptured proteins were eluted from the immune complexes using neutral pH elution buffer.

2.5.2. Size-exclusion chromatography (SEC)

Immunoaffinity-purified protein extracts were loaded on a Superdex 75 (10/300 GL) column (GE Healthcare) and eluted at a flow rate of 1 mL/min into 1 mL SEC fractions using 50 mM ammonium acetate, pH 8.5. Fractions of eluate were concentrated approximately 10-fold using YM-3 Centriprep filters (Millipore). Half of each fraction was frozen within 1–2 min of collection and stored at −80 °C. The other half were electrophoresed on 4–12–15% SDS/PAGE gels, and the separated proteins were then transferred to nitrocellulose membranes and immunoblotted with 4G8 antibodies (1:1000) to identify the types of oligomers.

2.5.3. Protein concentrations

Protein amounts were determined using a BCA ProteinAssay (Thermo Scientific). For western blots, 10 μl of protein extracts was incubated for 1 h at 37 °C.

2.6. Primary cell cultures

2.6.1. Neuronal cultures

Primary cortical cells were isolated from 16-day-old mouse embryos (C57BL/6 or apoE$^{-/-}$ mice).Trypsin (2.5%)was then added, and the cells were incubated for 30 min. The trypsin solution was gently removed, and DMEM/F-12 mediumwas added. The cells were allowed to incubate for 5 min at room temperature. Cortices were homogenized by repeatedly pipetting them up and down using a pipette until a homogeneous tissue suspension was achieved. The homogeneous tissue suspension was transferred to a pre-equilibrated 100 μm cell strainer and the flow-through was collected in a conical tube. The obtained cells were plated on poly-L-lysine (Sigma-Aldrich)-coated coverslips in 35 mm dishes at a density of 10^5 cells/dish or in a 6-well cell culture cluster at a density of 1.5×10^5 cell/cm^2 in DMEM/F-12 medium with 10% fetal bovine serum. After 4 h, the medium was replaced with neurobasal medium supplemented with 2% B27 and 0.5 mM GlutaMAX-I. Cells were grown in medium with 5 μM Ara-C for neuronal cultures. After the cells were submitted to 48 h of Ara-C treatment (in primary neuron culture), the medium was replaced with neurobasal medium supplemented with 2% B27and 0.5 mM GlutaMAX-I. At the start of all experiments, the cultures were maintained for 7 or 14 days. The experiments were performed on near-pure neuronal cultures (> 98% immunoreactive cells as assessed by the expression of MAP-2).

2.6.2. Astrocyte cultures

Cortices isolated from neonatal C57BL/6J or apoE$^{-/-}$mice (1- to 2-day-old) were mechanically dissociated. The method used to homogenize the cortices wasthe same as that used for neuronal cultures. The obtained cells were plated on poly-L-lysine-coated flasks in DMEM/F-12 medium with 10% fetal bovine serum. After 14 days, oligodendrocytes and microglia were removed from the mixed glia cultures by a differential shaking and adhesion procedure, and the astrocytes were collected from the flasks by trypsinization. The cells were plated in either 6-well plates (1.5×10^5 cells/well) or 35-mm dishes (10^5 cells/dish) coated with poly-L-lysine. To reduce microglial growth, the culture medium was changed every second day. Astrocytes were cultured for at least 1 month before carrying out experiments. The cultures routinely contained 98% astrocytes as assessed by expression of the astrocyte marker GFAP antibody.

2.6.3. Cocultures

Neurons to be grown in cocultures were plated onto coverslips in 12-well plates at a concentration of 15×10^4 cells/cm^{2}inneurobasal medium supplemented with 2% B27 and 0.5 mM GlutaMAX-I. After 7 days, astrocytes previously maintained in culture for 21 days were added to these neurons at a density of 100×10^4 cells/mL. Cocultures were grown for an additional 7 days before commencing the analysis.

2.7. Preparation of astrocyte-conditioned medium (ACM) and AβO-preactivated ACM

Astrocyte cultures were grown in the medium containing DMEM/F12 and neurobasal medium (1:1) and 2% B27 supplement. After 24 h, the medium was replaced with neurobasal medium supplemented with 2% B27 and 0.5 mM GlutaMAX-I. The astrocytes were grown in medium with or without 5 μM AβOs to obtain AβO-preactivated ACM and control ACM, respectively.

2.8. AβOs stimulation and BACE1 inhibitor treatment

The cocultures, pure astrocytes or neurons were treated with 5 μM AβOs (extracted from 15- to 24-month-old PS1V97L-Tg mouse brains) for 24 h, 48 h or 72 h. Controls received fresh cell culture medium without AβOs. After AβOs treatment, the cells were fixed or lysed. For BACE1 inhibitor treatment, the primary astrocytes were treated with 1 μM LY2886721 dissolved in DMSO. Control assays were performed using DMSO. After 2 h, the astrocytes were treated with 5 μM AβOs for 24 h.

2.9. Cell medium and lysates

The neurons and astrocytes were cultured at a concentration of 1.5 x 10^5cells/cm^2 in cell culture dishes. To analyze the Aβ concentration in the media, the primary cells were exposed to 5 μM AβOs for 24 h. Controls received fresh cell culture medium without AβOs. Following 24 h of treatment, the cells were washed in cell culture media three times and cultured for an additional 24 h, 48 h or 72 h in Aβ-free cell culture medium. The neurons and astrocytes were lysed through a 1 mL sterile plastic syringe slowly up and down at least 5 times in ice-cold lysis buffer (20 mM Tris pH 7.5, 0.5% TritonX-100, 2% SDS, 0.5% deoxycholic acid, 150 mM NaCl, 10 mMEDTA, 30 mM NaPyroP and protease inhibitor (Roche), and incubated on ice for 30 min, then centrifuged to collect the supernatant (15 min, 4 °C, 12000 ×g). The medium and supernatants of cell lysates were stored at −80 °C until the time of analysis by ELISA or Western blot.

2.10. Cytotoxicity assays

Cytotoxicity was evaluated by measuring lactic dehydrogenase (LDH) levels in culture medium using a Cytotoxicity Detection Kit (Roche) according to the manufacturer's directions. After the medium was collected, the remaining cells were lysed in 2% (*w*/*v*) Triton X-100, and the LDH content in the medium and lysed cells was measured to determine the total LDH content. Absorbance was measured at 490 nm. LDH release from cells was calculated as a percentage of total LDH in each sample.

2.11. Aβ ELISAs

The expression levels of Aβ40 and Aβ42 in the mouse brain and cell media were determined using ELISA kits (IBL). Detection was carried out according to the manufacturer's instructions, and each sample was tested in triplicate.

2.12. Immunocytochemistry

The primary cell cultures on coverslips were fixed and permeabilized with 4% paraformaldehyde and 0.3% Triton X-100 for 30 min at room temperature. The cells were then washed with PBS three times and blocked with 10% normal goat serum for 1 h. The cells were incubated with the following primary antibodies overnight at 4 °C: mouse monoclonal anti-Aβ (4G8, 1:500), chicken polyclonal anti-GFAP (1:500), mouse monoclonal anti-GFAP (1:500), and rabbit monoclonal anti-MAP2 (1:800). The secondary antibodies were IgG conjugated to Alexa Fluor 488 or Alexa Fluor 594 (against rabbit, mouse or chicken IgG (Thermo Scientific)). The cell was incubated with secondary antibodies for 1 h at room temperature. Nuclei were stained with the fluorescent dye 4′,6-diamidino-2-phenylindole (DAPI) (Thermo Scientific). Finally, the cells were mounted on slides, and images were acquired with a Leica fluorescence microscope.

2.13. Analysis of neuronal morphology and Aβ integral optical density and cell counting

The morphologies of neurites were indicated based on immunostaining for MAP2. Using exactly the same settings, the images from three independent cultures were captured with a x20 objective on a Leica microscope. We used ImageJ software to measure neuronal process outgrowth, and the longest length of each neuronal process was traced. The integral optical density of Aβ immunoreaction was analyzed with ImageJ software. All integral optical density for Aβ was set manually in the software, and the number of viable cells was determined by manually counting cell nuclei in each field. All experiments were repeatedly at least 3 times in a blinded fashion.

2.14. Western blot analysis

Samples were loaded for SDS/PAGE [4–12% or 4–12–15% (*w*/*v*) acrylamide], and separated proteins were transferred to nitrocellulose membranes. The membranes were blocked in a solution of 5% fat-free milk for 30 min at 20 °C and incubated overnight at 4 °C with one of the following primary antibodies: GFAP (1:1000), MAP2 (1:1000), apoE (1:1000), A11 (1:500), sAPPβ (1:1000), BACE1 (1:1000), Aβ (6E10 and 4G8, 1:1000), or β-actin (1:3000). After incubation with the primary antibody, the samples were incubated at 37 °C for 1 h with HRP-labeled secondary antibodies and then visualized using enhanced chemiluminescence reagents (Milipore). The membranes were scanned (Alpha Innotech, USA), and optical densities were determined using ImageJ software. The band densities were all normalized to β-actin.

2.15. Statistics

The results are presented as the mean ± SEM. For the MWM learning test, we used univariate repeated measures ANOVA to analyze the dataforescapelatency. The other statistical analyses were performed using either Student's *t*-test (two-group comparison) or one-way ANOVA (more than two groups) followed by Bonferroni's post hoc comparison. $p < .05$ was considered significant.

3. Results

3.1. Nonameric and dodecameric Aβ assemblies induced cognitive impairment in PS1V97L-Tg mice

In previous studies, we discovered that pathological alterations in the intraneuronal accumulation of AβOs occurred without Aβ plaques in PS1V97L-Tg mice, and strong evidence showed that AβOs were responsible for age-related memory decline [18]. However, the soluble AβOs include a series of Aβ assemblies, and the pathogenicity of each AβO species may be different. To assess the causal effects exerted by different Aβ assemblies on memory decline, we observed the dynamic change in Aβ assemblies during the process of cognitive impairment in 6- to 15-months-old PS1V97L-Tg mice.

First, we evaluated the cognitive profiles of PS1V97L-Tg mice aged from 6 to 15 months old in the Morris water maze (MWM) test. With increasing training days, the escape latency in all groups gradually decreased except in the 15-month-old PS1V97L-Tg mice. The escape latency was significantly longer in 9-month-old PS1V97L-Tg mice than 6-month-old Tg mice and wild type (WT) mice on the third training day (Fig. 1a). Spatial memory was further evaluated in the probe trial performed by removing the platform after 5 training days. Compared with the 6-month-old PS1V97L-Tg mice, the 9-month-old Tg mice showed a significant decrease in dwelling time in the target quadrant, and this discrepancy gradually increased in 15-month-old Tg mice (Fig. 1b). In addition, we did not find any difference in swimming speed on the first training day among these groups (Fig. 1c), and this excluded any potential influence of motor disabilities on escape latency.

We then investigated age-dependent changes in AβOs the brains of PS1V97L-Tg mice. Immunoblotting of the brain extracts showed that there was a set of apparent assemblies of Aβ in the PS1V97L-Tg mice brains, but not in the WT mice brains (Fig. 1d). In addition to a faint 4 kDa band corresponding to the Aβ monomer, 4G8 immunoreactive proteins were detected at molecular mass theoretically corresponding to trimeric (14 kDa), tetrameric (18 kDa), nonameric (40 kDa) and dodecameric (56 kDa) Aβ assemblies. The nonamer and dodecamer significantly increased in the 9-month-old Tg mice compared with the 6-month-old Tg mice, and this discrepancy was most significant in the 15-month-old Tg mice (Fig. 1e, f). The trimer and tetramer did not significantly change with advancing age in the PS1V97L-Tg mice (Fig. 1g, h). We evaluated the natural AβOs with the anti-oligomer antibody A11 (Fig. S.1a), which specifically detected only 27–56 kDa complexes [8]. The brain protein of PS1V97L-Tg mice were fractionated by immunoprecipitation of 4G8 antibody and non-denaturing SEC, subjected to SDS–PAGE. High- and low-molecular-mass Aβ assemblies (at expected intervals) were collected in different fractions, arguing against the possibility that SDS or self-oligomerization triggered the formation of the AβOs.

In MWM test, we found the cognitive impairment in 9-month-old Tg mice, which was more severe along with the growth of age. The nonamer and dodecamer appeared before cognitive impairment, and their expression gradually increased with the deterioration of cognitive impairment. These findings suggest that nonameric and dodecameric Aβ assemblies may be the main molecules that induce memory decline. Next, we purified the Aβ assemblies obtained from 15 to 24-month-old PS1V97L-Tg mice brains using immunoprecipitation (with 4G8 antibody), and separated each Aβ assembly using size exclusion chromatography to detect their cytotoxicity in primary mixed culture. The results showed that only the nonamer and dodecamer were associated with significantly increased lactate dehydrogenase (LDH) release at 12 h (Fig. S.2).

We also examined soluble Aβ40 and Aβ42 concentrations in the brain tissues using ELISA, and found Aβ40 and Aβ42 were significantly increased in the brains of the PS1V97L-Tg mice than in their WT littermates at 6-months-old ($p < .01$), and this discrepancy progressively escalated in the older mice (Fig. 1i, j).

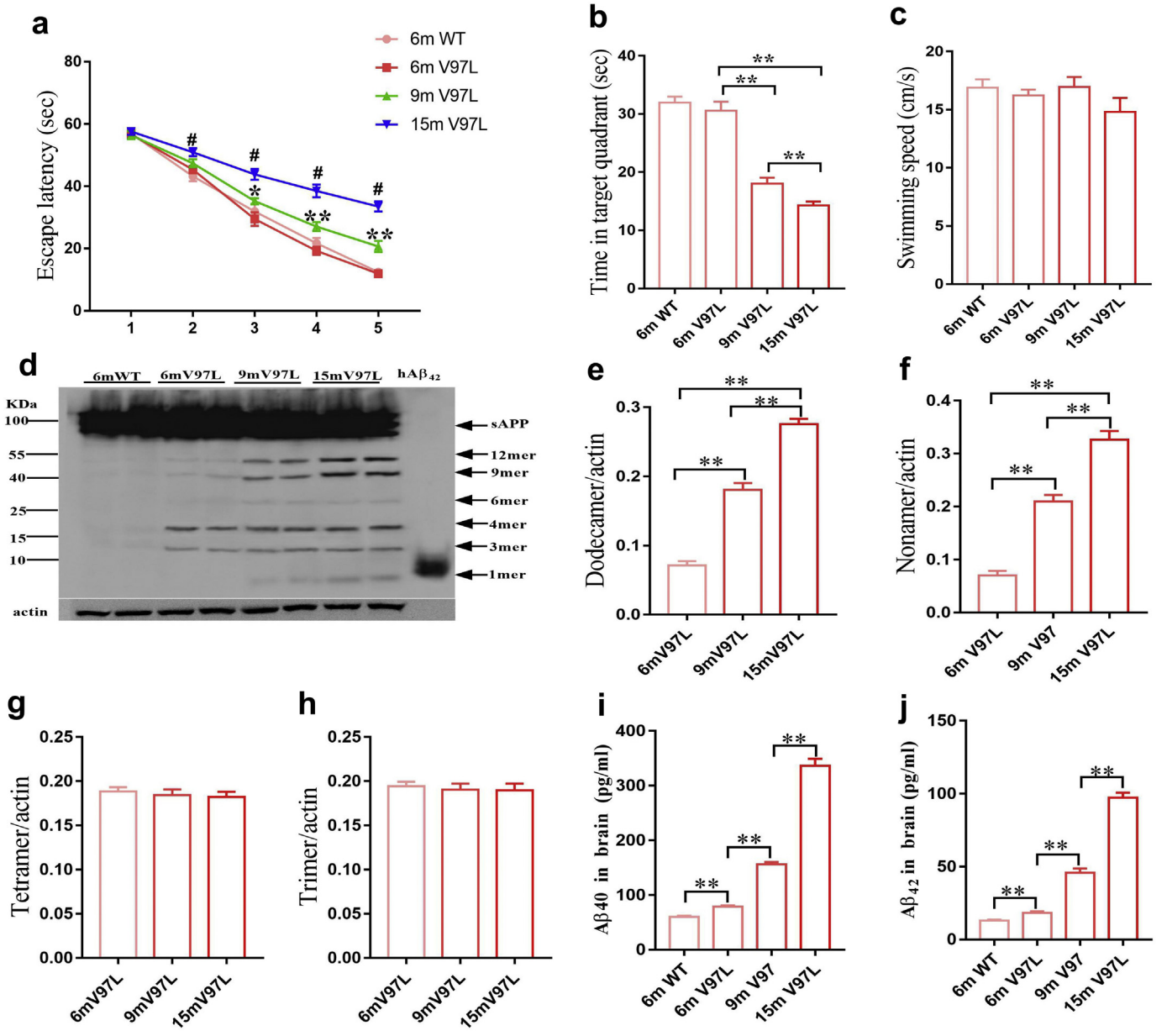

Fig. 1. Temporal patterns of soluble Aβ assemblies and cognitive impairment in PS1V97L-Tg mice. (a-c) Representative MWM analysis of 6- to 15-month-old PS1V97L-Tg mice. (a) MWM escape latency during training (ANOVA with repeated measures, $F = 33.298$, $p < .0001$, $n = 12$/group). (b) Time in the target quadrant (one-way ANOVA, $F = 62.16$, $p < .0001$, $n = 12$/group). (c) Swimming speed on the first training day (one-way ANOVA, $F = 1.337$, $p = .2745$ n = 12/group). (d) Identification of AβOs in soluble proteins obtained from the brains of 6-, 9-, and 15-month-old mice (age indicated above the lanes) by 4G8 monoclonal antibodies. The synthetic human Aβ42 peptide (hAβ42) was used as a size marker and positive control. The right lane indicates the respective migration positions of monomers (1mer), trimers (3mer), tetramers (4mer), hexamers (6mer), nonamers (9mer), dodecamers (12mer) and sAPP. (e-h) Bar graphs illustrate the protein expression levels of trimers, tetramers, nonamers and dodecamers in the brains of PS1V97L-Tg mice (one-way ANOVA, 12mer: $F = 167.2$, $p < .0001$, 9mer: $F = 98.48$, $p < .0001$, 4mer: $F = 0.3061$, $p = .7408$, 3mer: $F = 0.138$, $p = .8722$, $n = 6$/group). (i, j) Aβ40 and Aβ42 expression levels measured by ELISA (one-way ANOVA, i: $F = 320.4$, $p < .0001$; j: $F = 280.9$, $p < .0001$, $n = 6$/group). The data are shown as the mean ± SEM; $*p < .05$, $**p < .01$, $^{\#}p < .01$ compared with the WT group.

3.2. Toxic AβOs were duplicated and amplified in astrocyte triggering neuronal injury

We compared the cytotoxicity of natural AβOs in the primary cocultures containing both neurons and astrocytes. LDH release was used to measure cellviability. Treatment of the cultures with natural AβOs (5 μM) resulted in a significant increase in LDH release at 24 h, 48 h and 72 h (Fig. 2a.1). In contrast, the same dose of AβOs did not induce the release of LDH in the primary neuron or primary astrocyte culture after 24 h to 72 h (Fig. 2b,1, 2). To identify the source of this LDH, we stimulated the mixed cultures with AβOs for 48 h, and labeled astrocytes with GFAP antibody (green), and neurons with MAP2 antibody (red). We found that compared with controls, in the treated cells, neurons were severely damageddemonstrated by the loss of synapses, dissolved axons dissolving, lower fluorescence intensities and unclear outlines. In contrast, while astrocytes exhibited stellate morphologies under control conditions, following exposure to AβOs, they showed clear and robust alterations in morphology, including cell body hypertrophy and proliferation (Fig. 2b). These changes are thought to represent the characteristics of reactive astrogliosis [16,22,23], which could induce the secretion of inflammatory cytokines (Fig.S.3). Immunoblotting showed that the expression of MAP2 was decreased and GFAP was increased in a time-dependent manner from 24 h to 48 h (Fig. 2c–e). These results indicate that neurons, rather than astrocytes,

are susceptible to the toxicity caused by AβOs. The astrocytes were activated in response to AβOs, and this event was closely associated with Aβ-induced neuronal death. To further confirm that astrocytes are important mediators of Aβ-induced neurotoxicity, we cultured neurons in astrocyte conditioned medium (ACM) with AβOs or ACM from preactivated astrocytes exposed to AβOs for 48 h. We found that the AβOs preactivated ACM strongly induced neurotoxicity (Fig. 2f). Remarkably, neurons were more susceptible to the AβOs preactivated ACM toxicity, as shown by the loss of synapses and shorter axons (Fig. 2g).

To investigate the mechanism underlying AβOs induced neuronal injury in the cocultures, we incubated the primary astrocytes and neurons with the same concentrations of AβOs for 48 h, and then labeled the astrocytes with GFAP antibody, neurons with MAP2 and Aβ with 4G8 antibody. Interestingly, there was no fluorescence of Aβ in the primary astrocytes. After incubation with AβOs for 48 h, there was significant AβOs (red) deposition around perinuclear endochylema of astrocytes (Fig. 3a). Immunoblotting the astrocyte lysates (Fig. 3b), the level of 4G8 immunoreactive proteins were very faint in the astrocytes. However, after AβOs treatment, a set of 4G8 immunoreactive bands became significant, including those at molecular mass theoretically corresponding to trimeric, nonameric and dodecameric Aβ assemblies. Furthermore, we found that the expressions significantly increased from 24 h to 72 h incubation with AβOs in a time-dependent manner (Fig. 3c–e). These results suggest that the natural AβOs are augmented in astrocytes. Conversely, no fluorescence for

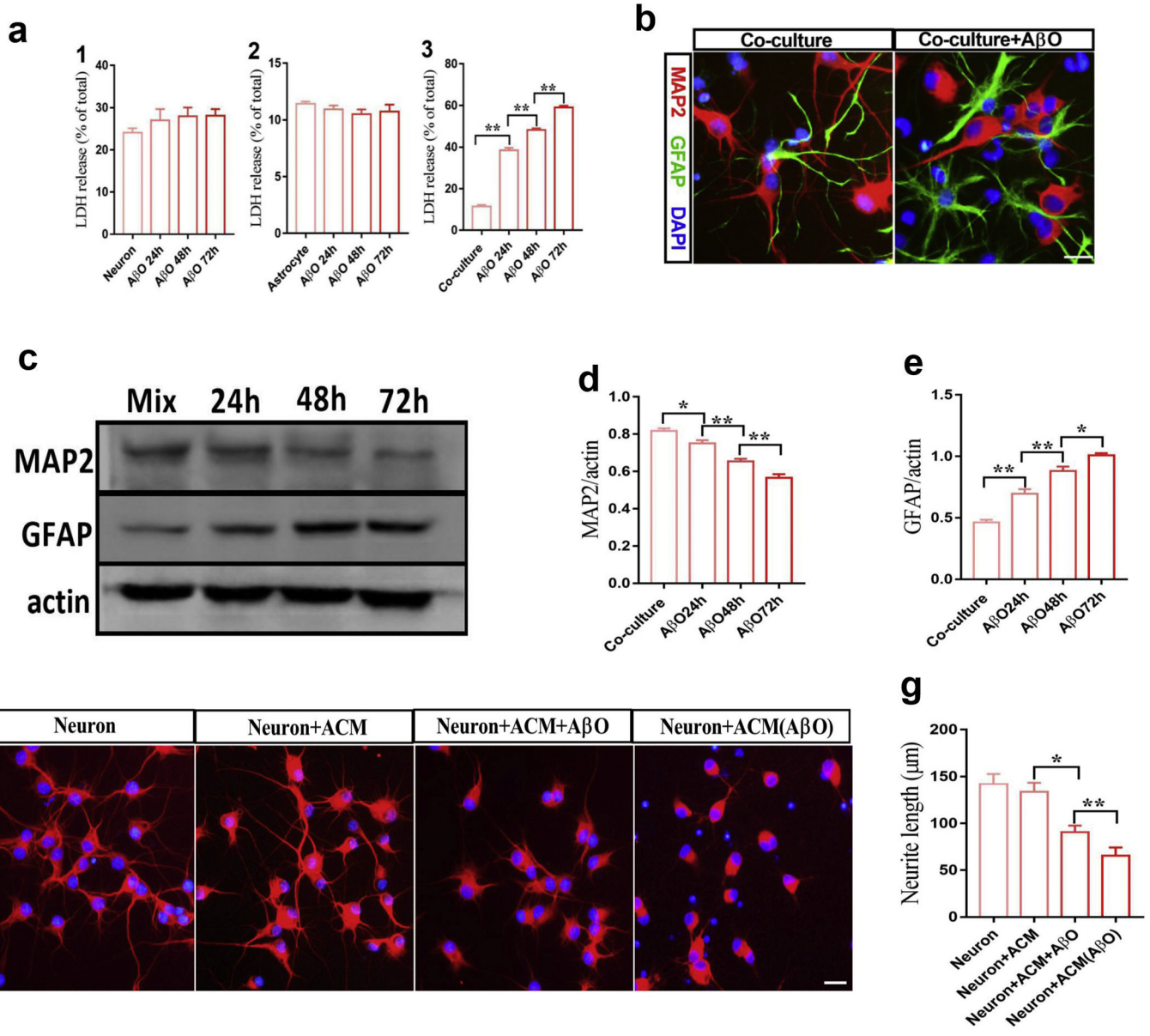

Fig. 2. Astrocytes are important mediators of Aβ-induced neurotoxicity. (a) Representative time-dependent effects of AβOs on LDH release. The cell viability of primary neurons, astrocytes and coculturesexposed to 5 μM AβOs for 24 h, 48 h and 72 h (one-way ANOVA, neuron: $F = 0.9174$, $p = .4504$; astrocytes: $F = 0.8352$, $p = .4903$; cocultures: $F = 490.5$, $p < .0001$; $n = 6$/group). (b) Representative images of cortical mixed cultures of neurons and astrocytes treated for 48 h with 5 μM AβOs and then immunolabelled with an antibody against GFAP (green) to label astrocytes or MAP2 (red) to label neurons. DAPI was used to stain nuclei (blue). (c) Western blot showing the expression of GFAP and MAP2 at 48 h in cocultures treated for 48 h with 5 μM AβOs; (d and e) Bar graphs illustrate the protein expression levels of MAP2 and GFAP (one-way ANOVA, d: $F = 46.33$, $p < .0001$; e: $F = 66.95$, $p < .0001$, $n = 6$/group); (f) Representative images of primary neurons cultured in astrocyte-conditioned medium (ACM) containing 5 μM AβO (ACM + AβOs) or preactivated ACM exposed to 5 μM AβOs for 48 h (ACM (AβOs)); the cells were then immunolabelled with MAP2 (red) to label neurons. DAPI was used to stain nuclei (blue); (g) Bar graphs illustrating the neurite lengths of neurons cultured in different conditioned media(one-way ANOVA, $F = 12.56$, $p < .0001$, $n = 6$/group); The data are shown as the mean ± SEM; $^{*}p < .05$, $^{**}p < .01$; Scale bar:50 μm.

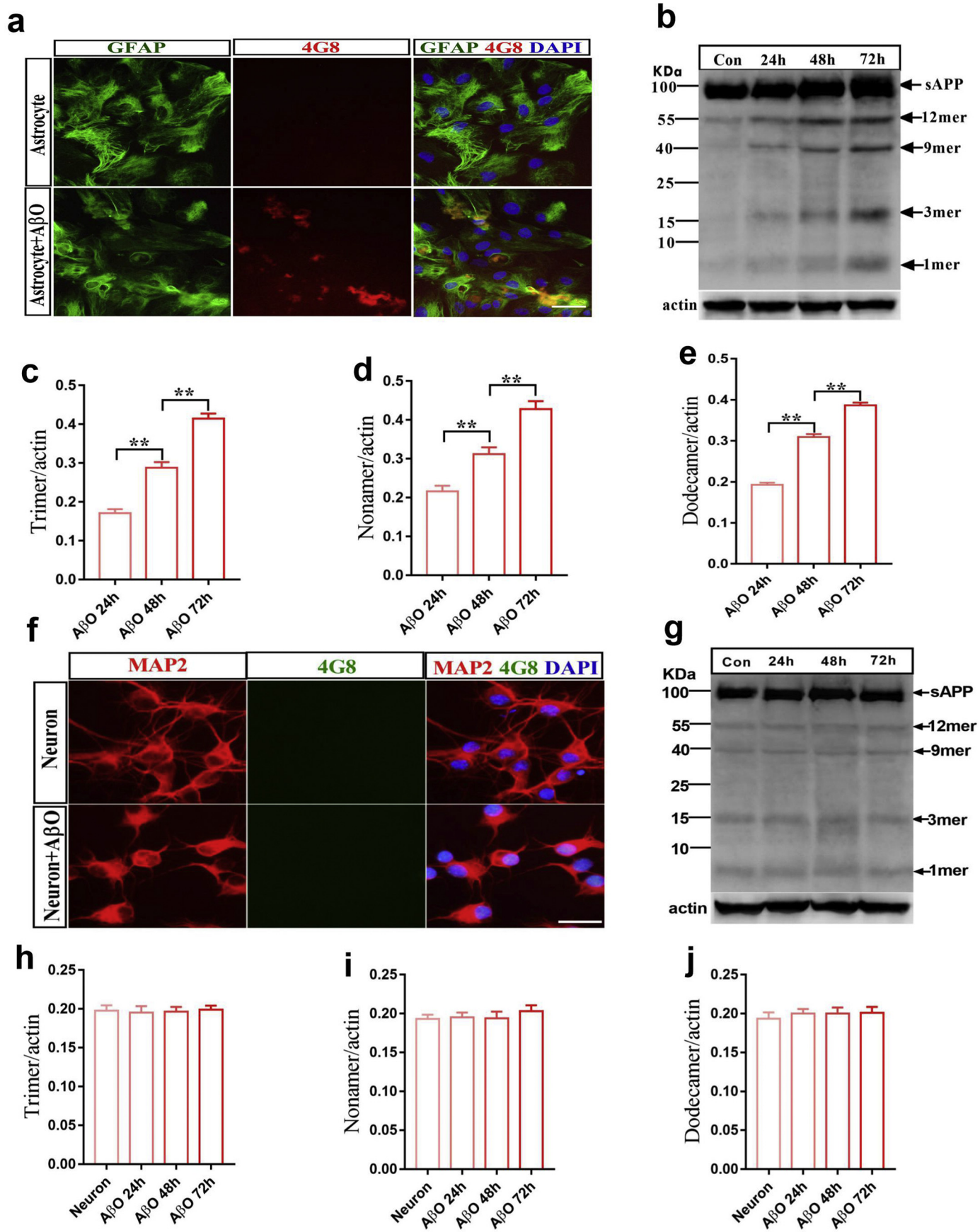
a
GFAP
4G8
GFAP 4G8 DAPI
Astrocyte
Astrocyte+AβO
b
Con
24h
48h
72h
KDa
100
55
40
25
15
10
sAPP
12mer
9mer
3mer
1mer
actin
c
Trimer/actin
0.5
0.4
0.3
0.2
0.1
0.0
**
**
AβO 24h
AβO 48h
AβO 72h
d
Nonamer/actin
0.5
0.4
0.3
0.2
0.1
0.0
**
**
AβO 24h
AβO 48h
AβO 72h
e
Dodecamer/actin
0.5
0.4
0.3
0.2
0.1
0.0
**
**
AβO 24h
AβO 48h
AβO 72h
f
MAP2
4G8
MAP2 4G8 DAPI
Neuron
Neuron+AβO
g
Con
24h
48h
72h
KDa
100
55
40
25
15
10
sAPP
12mer
9mer
3mer
1mer
actin
h
Trimer/actin
0.25
0.20
0.15
0.10
0.05
0.00
Neuron
AβO 24h
AβO 48h
AβO 72h
i
Nonamer/actin
0.25
0.20
0.15
0.10
0.05
0.00
Neuron
AβO 24h
AβO 48h
AβO 72h
j
Dodecamer/actin
0.25
0.20
0.15
0.10
0.05
0.00
Neuron
AβO 24h
AβO 48h
AβO 72h

4G8 was observed in the neurons incubated without or with AβOs incubation (Fig. 3f). Immunoblotting showed that there was a set of Aβ assemblies in the neuronal lysates (Fig. 3g). The expressions of trimeric, nonameric and dodecameric Aβ assemblies did not change among the neurons incubated without or with AβOs treatment from 24 h to 72 h (Fig. 3h–j).

3.3. AβOs induced amyloidogenic processing and the expression of apoE in astrocytes, but not neurons

Aβ peptides are mainly produced in cells expressing amyloid precursor protein (APP) via sequential scission by BACE1 and γ-secretase. BACE1 cleaves APP into the membrane-tethered C-terminal βfragments (CTFβ) and N-terminal secreted β-cleavage of APP (sAPPβ). CTFβ is subsequently cleaved by γ-secretases into an extracellular Aβ and APP intracellular domain. In this study, we found that treatment with natural AβOs increased the expression and activity of BACE1 in a time-dependently manner from 24 h to 72 h and induced the production of sAPPβ (Fig. 4a-c). Nonetheless, the expression of BACE1 and sAPPβ was not different between the neurons treated with or without AβOs (Fig. 4e–g). The expression of apoE was also induced in a time-dependent manner following AβOs treatment in astrocytes, but not neurons (Fig. 4d, h).

We examined Aβ40 and Aβ42 concentrations in the extracellular medium of primary neurons and astrocytes using ELISA test. The levels of Aβ40 and Aβ42 were very low in the media of primary neurons and astrocytes. However, after treatment with AβOs, the levels of Aβ40 and Aβ42 gradually increased from 24 h to 72 h (Fig. 4i, j) in the medium of primary astrocytes, but they did not change in the medium of primary neurons (Fig. 4k, l).

3.4. The natural AβOs induced cognitive impairment through time-dependent self-replication

To observe the effects of natural AβOs on learning and memory function, adult (3-month-old) male Sprague-Dawley rats were injected intracerebroventricular (i.c.v) injection. The MWM test was used to investigate the changes in behaviour at 20 days and 40 days after i.c.v. injection. For escape latency, compared to i.c.v. injection 20-day group and sham-operated group, the i.c.v. injection 40-day group showed significant impairment in the escape latency to find the hidden platform after the third training day (Fig. 5a). In the probe trial, the results demonstrated that the time spent in the target quadrant and the number of times crossing the platform were significantly lower in the i.c.v. 40-day group than in the sham-operated group and the i.c.v. 20-day group (Fig. 5b, c).

To investigate the mechanism by which Aβ assemblies induce cognitive impairment in rats, we investigated the dynamic change in Aβ assemblies at 20 and 40 days after i.c.v. injection. Immunoblotting the brain extracts, 4G8 immunoreactive proteins was detected in a set of faint bands with molecular masses theoretically corresponding to the monomeric, trimeric, nonameric and dodecameric Aβ assemblies in the brain of sham-operated group. While, the expression of the 4G8 immunoreactive bands significantly increased time-dependently after i.c.v. injection (Fig. 5d-h). Moreover, we found that natural Aβ oligomers time-dependently increased GFAP, sAPPβ, BACE1 and apoE expression in the brain of rats following i.c.v. injection (Fig. 5i–l). The expression of apoE was induced in a time-dependent manner after AβOs i.c.v. injection (Fig. 5m).

3.5. BACE1 is responsible for the natural AβOs induced redundant Aβ in astrocytes

To explore the mechanism of AβOs self-replication in astrocytes, we treated the primary astrocytes with AβOs in the presence or absence of the BACE1 inhibitor LY2886721. We incubated the natural AβOs in astrocytes with or without LY2886721 pretreatment astrocytes for 2 h. Pharmacological BACE1 inhibition led to a pronounced reduction in the level of sAPPβ in the lysates and a significant decrease in Aβ40 and Aβ42 levels in the extracellular medium of primary astrocytes (Fig. 6i–m). These results indicated that the activity of BACE1 was blockaded by LY2886721. Immunofluorescence showed that BACE1 inhibition significantly reduced the fluorescence for Aβ (red) in astrocytes (Fig. 6a–c). Immunoblotting of the primary astrocyte lysates revealed that treatment with natural AβOs significantly increased the expression of monomer, trimeric, nonameric and dodecameric Aβ assemblies, and this pathological process was effectively suppressed by pharmacological BACE1 inhibition (Fig. 6d–h). Hence, the BACE1 inhibitor effectively decreased the generation of AβO and at the same time decreased the release of LDH in the media of mixed cultures to protect the neurons from damage by Aβ oligomers (Fig. S.4).

3.6. ApoE is the key binding protein for Aβ assembly to form toxic AβOs (nonamer and dodecamer)

ApoE is a known Aβ binding protein and a genetic risk factor for AD [24,25], that is synthesized and secreted predominantly by astrocytes in the CNS. Our results also demonstrated that the natural AβOs increased the expression of apoE in astrocytes but not neurons in a time-dependent manner. We incubated synthetic Aβ42 with or without recombinant human apoE2, apoE3 or apoE4 protein to investigate the Aβ oligomerization assay in vitro. In the absence of apoE, Aβ assembly was only trimeric. In contrast, in the presence of apoE2, apoE3 or apoE4, the bands for Aβ nonamer and dodecamer gradually accumulated during the incubation period (Fig. S.5), especially in the apoE4 lane.

ApoE$^{-/-}$ astrocytes were treated with the natural AβOs for 24 h, and astrocytes were then labeled with GFAP antibody and Aβ with 4G8 antibody. There was pronounced 4G8 positive Aβ fluorescence (red) around the perinuclear endochylema (Fig. 7a). By immunoblotting the apoE$^{-/-}$ astrocyte lysates, 4G8 immunoreactive proteins were detected only at molecular mass of 4 kDa and 14 kDa bands, which corresponded to Aβ monomer and trimer after AβOs treatment (Fig. 7b–d). The results suggest that apoE may be crucial for enhancing the oligomerization of Aβ to form toxic oligomers (nonamer and dodecamer). Next, we treated apoE$^{-/-}$ astrocytes with natural AβOs for 24 h to observe changes in amyloidogenic processing. The results showed that the natural AβOs increased the expression of BACE1 and sAPPβ in the lysates and increased Aβ40 and Aβ42 levels in the medium of apoE$^{-/-}$ astrocytes (Fig. 7e–i). The cytotoxicity of natural AβOs was assessed by LDH release assays in apoE$^{-/-}$ mixed cultures. Strikingly, we found that treatment with AβOs (5 μM) did not induce the release of LDH in the apoE$^{-/-}$ mixed culture (Fig. S.6).

The apoE$^{-/-}$ mice undergoing i.c.v. injection of the natural AβOs, and the MWM test was used to investigate changes in behavior afer

Fig. 3. Toxic AβOs induced self-replication in astrocytes but not neurons. (a) Representative images of astrocytes treated for 48 h with 5 μM Aβ oligomers. Cells were fixed and immunolabelled with antibodies against GFAP (green) to label astrocytes or 4G8 (red) to label AβOs. DAPI was used to stain nuclei (blue). (b) Western blot showing the dynamic changes in Aβ assembly (4G8) observed in astrocytes treated with 5 μM AβOs; (c-e) Bar graphs illustrating the protein expression of trimers, nonamers and dodecamers in primary astrocytes (one-way ANOVA, c: $F = 86.79$, $p < .0001$; d: $F = 207.4$, $p < .0001$; e: $F = 221.1$, $p < .0001$; $n = 6$/group). (f) Representative images of neurons treated for 48 h with 5 μM AβOs; MAP2 (red) was used to label neurons, and 4G8 (green) was used to label AβO. DAPI was used to stain nuclei (blue). (g) Western blot showing dynamic changes inAβ assembly (4G8) in primary neurons treated with 5 μM AβOs. (h-j) Bar graphs illustrate the protein expression levels of trimers, nonamers and dodecamers in primary neurons (h: $F = 0.048$, $p = .985$; i: $F = 0.404$, $p = .751$; j: $F = 0.214$, $p = .886$, $n = 6$/group).The data are shown as the mean ± SEM; $*p < .05$, $**p < .01$; scale bar: 50 μm.

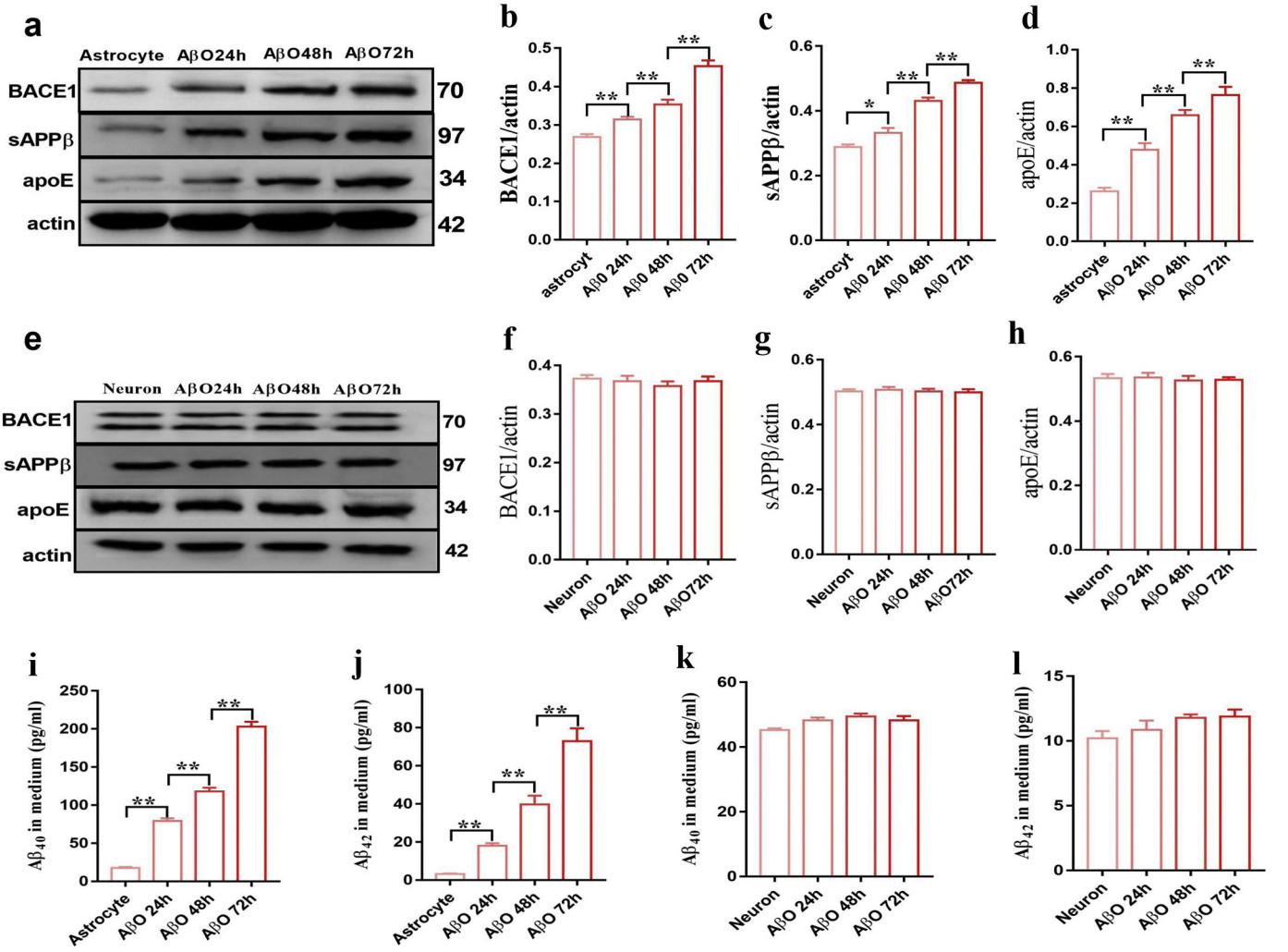

Fig. 4. Natural AβOs induced amyloidogenic processing in astrocytes. Western blots and quantitative analysis showing BACE1, sAPPβ and apoE levels in primary astrocyte (a) and neuron (e) cultures. Bar graphs illustrating the protein expression levels of BACE1, sAPPβ and apoE in primary astrocyte (b-d) and neuron (f-h) (one-way ANOVA, b: $F = 52.03$, $p < .0001$, c: $F = 69.79$, $p < .0001$, d: $F = 46.81$, $p < .0001$, f: $F = 0.436$, $p < .729$, g: $F = 0.143$, $p = .933$, h: $F = 0.126$, $p = .943$, $n = 6$/group). The levels of Aβ40 and Aβ42 in the medium obtained from astrocytes or neurons (i-l) (one-way ANOVA, i: $F = 310$, $p < .0001$, j: $F = 53.06$, $p < .0001$, k: $F = 2.73$, $p = .051$, l: $F = 2.11$, $p = .132$, $n = 6$/group). The data are shown as the mean ± SEM; $^{*}p < .05$, $^{**}p < .01$.

20 and 40 days. The results of MWM showed that the i.c.v. injection with AβOs didn't impair the spatial learning and memory in apoE$^{-/-}$ mice after 20 and 40 days AβOs (Fig. 8a–c). We next investigated dynamic changes in Aβ assemblies in i.c.v. injected apoE$^{-/-}$ mice. By immunoblotting the brain extracts, 4G8 immunoreactive proteins were mainly detected at molecular weight theoretically corresponding to 4 kDa and 14 kDa bands corresponding to Aβ monomers and trimers (Fig. 8 d). The expression of the Aβ monomers and trimers gradually increased after i.c.v. injection of AβOs in a time-dependent manner (Fig. 8e, f). The expression of toxic AβOs (nonamer and dodecamer) was very faint and almost undetectable. Moreover, the natural AβOs increased GFAP, BACE1 and sAPPβ expression in a time-dependent manner after i.c.v. injection (Fig. 8g, j).

4. Discussion

In the present study, we provide direct experimental evidence for the major pathogenic AβO species and investigate their production and spread. Using the PS1V97L-Tg mouse model, we show that nonameric and dodecameric Aβ assemblies are predominantly responsible for instigating neuronal injury and cognitive deficits. In addition, we found that toxic AβOs (nonamer and dodecamer) were duplicated in a time-dependent manner in astrocytes but not neurons, and the BACE1 and apoE proteins were responsible for this self-replicating effect.

In previous studies, intracerebral injections of synthetic Aβ that included mixtures of amyloid-β fibrils, protofibrils, oligomers and monomers in indeterminate proportions exerted the deleterious effects on learned behavior in rats [26,27]. However, an enduring barrier to understanding the pathogenicity of various Aβ assemblies is the difficulty in specifying and controlling their size and aggregation states. In this study, we sough to identify the specific species of natural Aβ assemblies that induce memory decline in the brains of PS1V97L-Tg mice aged from 6 to 15-months-old. We envisioned the candidate AβO molecules would meet two criteria for impairing memory. First, they should be present before cognitive impairment appears. Second, their levels should increase gradually with the deterioration of cognitive impairment. Because the nonameric and dodecameric Aβ assemblies appeared in 6-month-old Tg mice and significantly increased from 9-15monthsold, they fulfilled the criteria and are therefore the candidate Aβ assemblies that could cause memory deficits. In vitro studies also showed that only nonameric and dodecameric Aβ assemblies significantly increased LDH release. Trimer and tetramer were excluded as candidate AβOs, because their expressions did not change with the cognitive decline caused by aging in mice. In our previous study, we found

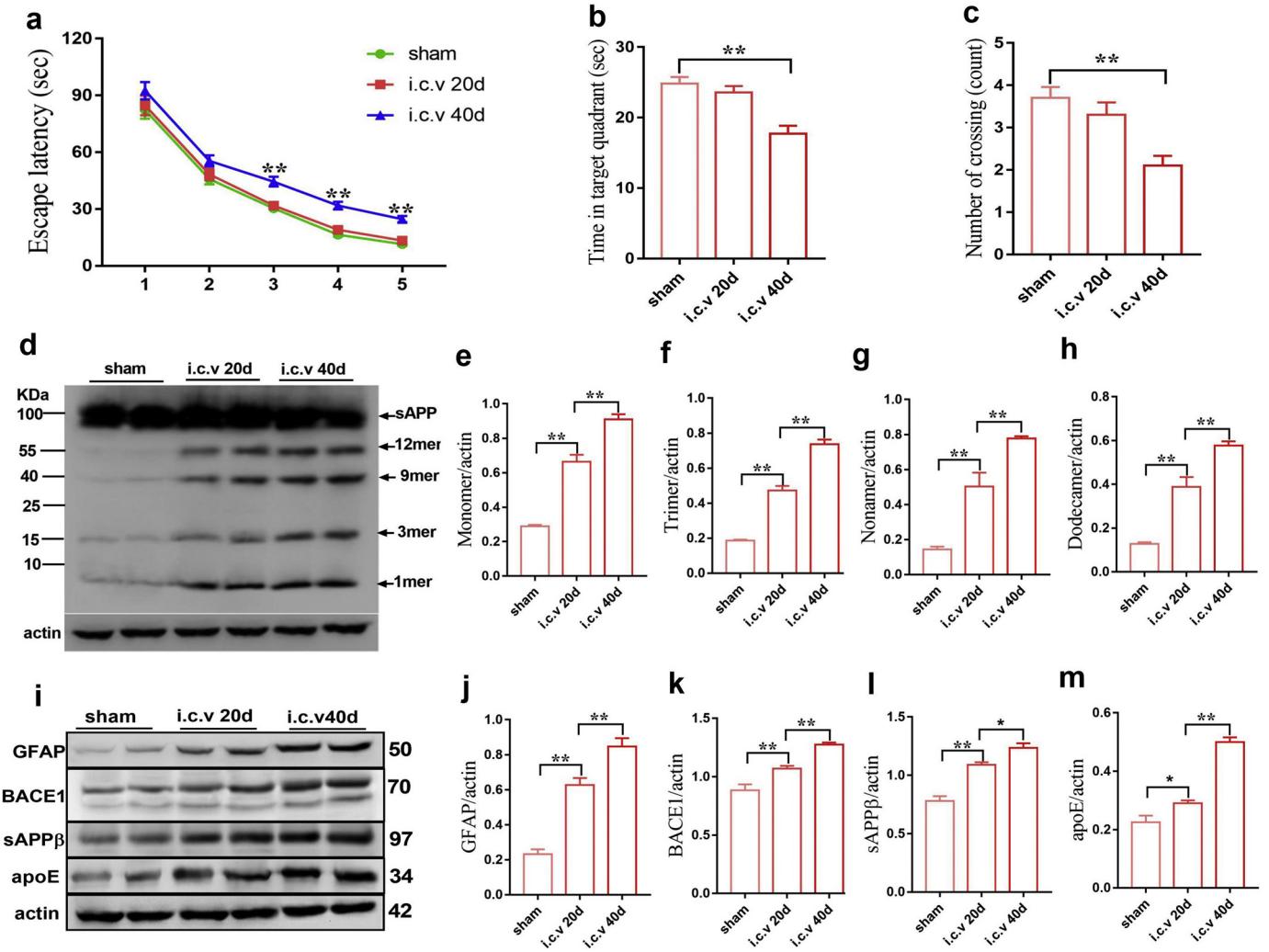

Fig. 5. Natural AβOs injection induced behavioral and biochemical changes in SD rats. (a) MWM escape latency during training (one-way ANOVA, F = 29.34, p < .0001; n = 10/group). (b) Time in the target quadrant (one-way ANOVA, F = 14.79, p < .0001, n = 10/group). (c) The number of crossings (one-way ANOVA, F = 9.81, p = .0006, n = 10/group). (d) Western blot showing dynamic changes in Aβ assembly (4G8) in the brains of SD rats (time indicated above the lanes). The right lanes indicate the respective migration positions of monomers, trimers, nonamers, dodecamers and sAPP. (e-h) Bar graphs illustrating the quantitative analysis of monomers, trimers, nonamers and dodecamers (one-way ANOVA, e: F = 108.3, p < .0001; f: F = 164.9, p < .0001; g: F = 45.89, p < .0001; h: F = 61.43, p < .0001; n = 6/group). (i) Western blots showing the expression of GFAP, BACE1, sAPPβ and apoE in rat brains. (j-m) Bar graphs illustrating the quantitative analysis of the Western blot results (one-way ANOVA, j: F = 61.83, p < .0001; k: F = 31.09, p < .0001; l: F = 41.37, p < .0001; m: F = 72.38, p < .0001; n = 6/group). The data are shown as the mean ± SEM; *p < .05, **p < .01.

that insoluble (the FA-soluble fraction) Aβ species were below the lower limit of detection in the brain tissues of PS1V97L-Tg mice [20].

While the mechanism by which Aβ pathology spreads in the AD brain has been debated for many years [28,29], the cellular mechanism underlying the production and spread of Aβ aggregation remains unclear. A clue to its onset may be the peculiar distribution of AβOs and activated astrocytes in the very early stages of pathology [10,30,31]. If we could improve our understanding of the relationship between AβOs and activated astrocytes, we might have a better handle on the etiology of AβOs. In the present study, we found that 5 μM AβOs were insufficient to injure neurons or astrocytes by themselves, but the same concentration of AβOs resulted in a significant increase in LDH release in cocultures and induced the neuronal injury. Our results also showed that neurons were more susceptible to the toxicity of AβOs preactivated ACM than the same concentration of AβOs applied with ACM, because the AβOs had been duplicated and produced in AβOs preactivated ACM. In vivo study, we found that exogenous AβOs activated astrocytes and augmented Aβ assemblies in a time-dependent manner until the rats developed cognitive impairment. As the numberof AβOs increased, more astrocytes were activated, and this created a vicious cycle resulting in deterioration of cognitive impairment. Our results demonstrate a novel molecular mechanism by which astrocytes accelerated Aβ-induced neuronal toxicity by augmenting toxic AβOs (nonamer and dodecamer). Thus, activated astrocytes may play a vital role in the initiation and progression of AD.

It used to be thought that neurons were the only cell type which expressed high levels of BACE1 and the only cells capable of producing Aβ [32,33]. However, BACE expression has been observed in reactive astrocytes around amyloid plaques. The number of these BACE1-positive reactive astrocytes was higher in AD patients than in older-age controls, particularly in the entorhinal cortex [34]. Astrocytes are the most numerous cell types in the brain, and even a small level of astrocytic Aβ production could make a significant contribution to neurological and neurodegenerative diseases [12]. Therefore, astrocytes have received a great deal of attention in analyses of AD pathological progression. In an attempt to identify the cellular mechanisms undering the duplication and production of AβOs in astrocytes, we investigated the expression of BACE1 and sAPPβ in astrocytes and neurons, because they are key enzymes in amyloidogenic processing and the BACE1 cleavage product. The results showed that natural AβOs could activate astrocytes and induce the expression of toxic AβOs, BACE1 and sAPPβ in a time-dependent manner, and this pathological process was effectively

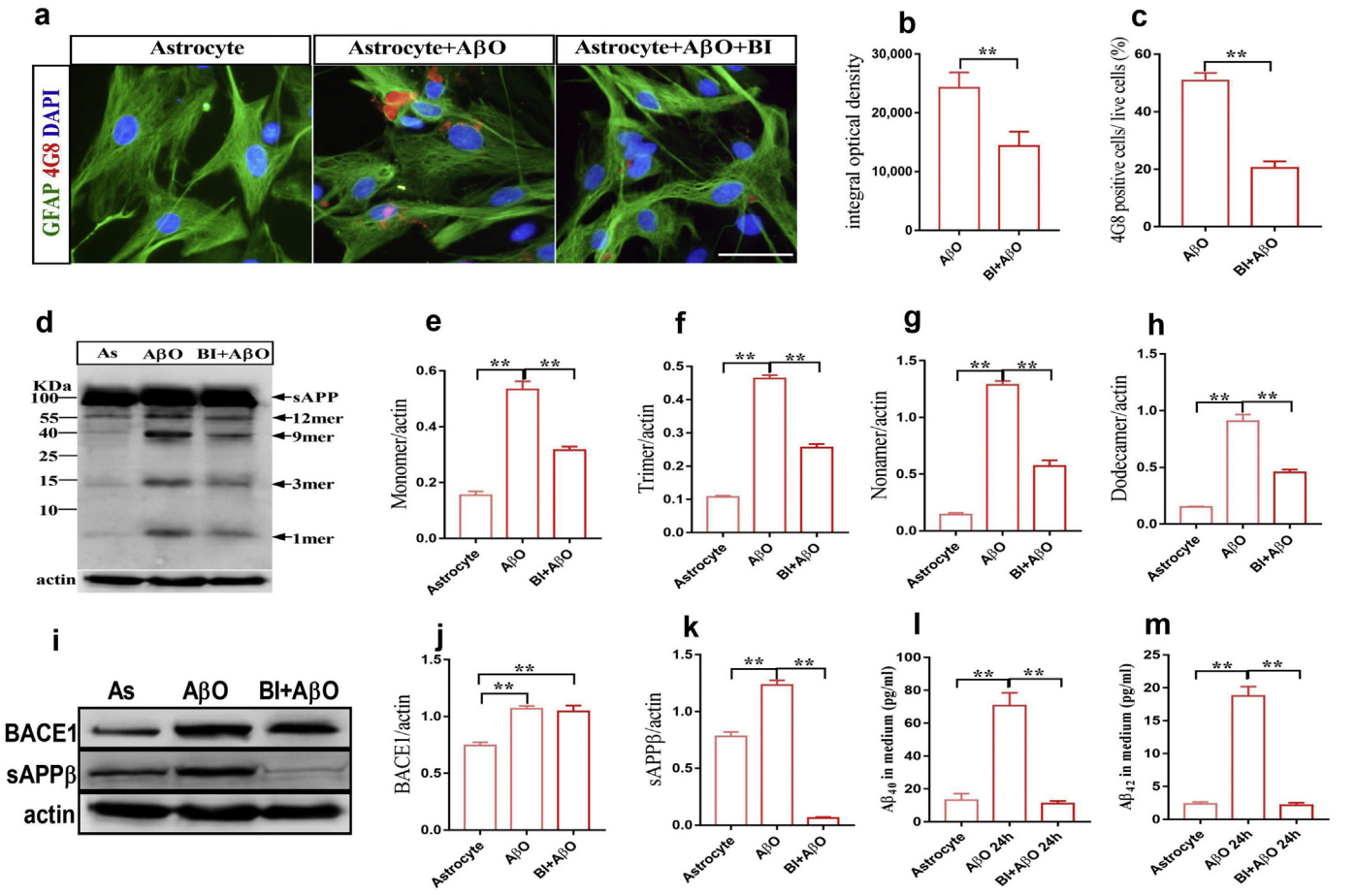

Fig. 6. BACE1 is responsible for the natural AβOs induced Aβ production in astrocytes. (a) Representative images from primary astrocyte cultures treated with 5 μM AβOs for 24 h or advanced 2 h treatment with BACE1 inhibiter (BI) then treated with 5 μM AβOs for 2 4 h; (b and c) Bar graphs illustrate the integrated optical density and 4G8 positive cells (*t*-test, b: $p = .0143$; c: $p < .0001$; $n = 5$/group); (d–h) Western blots and quantitative analysis for different Aβ assemblies; (one-way ANOVA, e: $F = 91.85$, $p < .0001$; f: $F = 428.7$, $p < .0001$; g: $F = 241.7$, $p < .0001$; h: $F = 106.1$, $p < .0001$; n = 6/group). (i–k) Western blots and quantitative analysis for BACE1 and sAPPβ (one-way ANOVA, j: $F = 24.05$, $p < .0001$; k: $F = 317.3$, $p < .0001$; n = 6/group); (l and m) The level of soluble Aβ40 and Aβ42 in the medium (one-way ANOVA, l: $F = 263.6$, $p < .0001$; m: $F = 118.8$, $p < .0001$; n = 6/group). The data are shown as the mean ± SEM, $^{*}p < .05$, $^{**}p < .01$; scale bar: 50 μm.

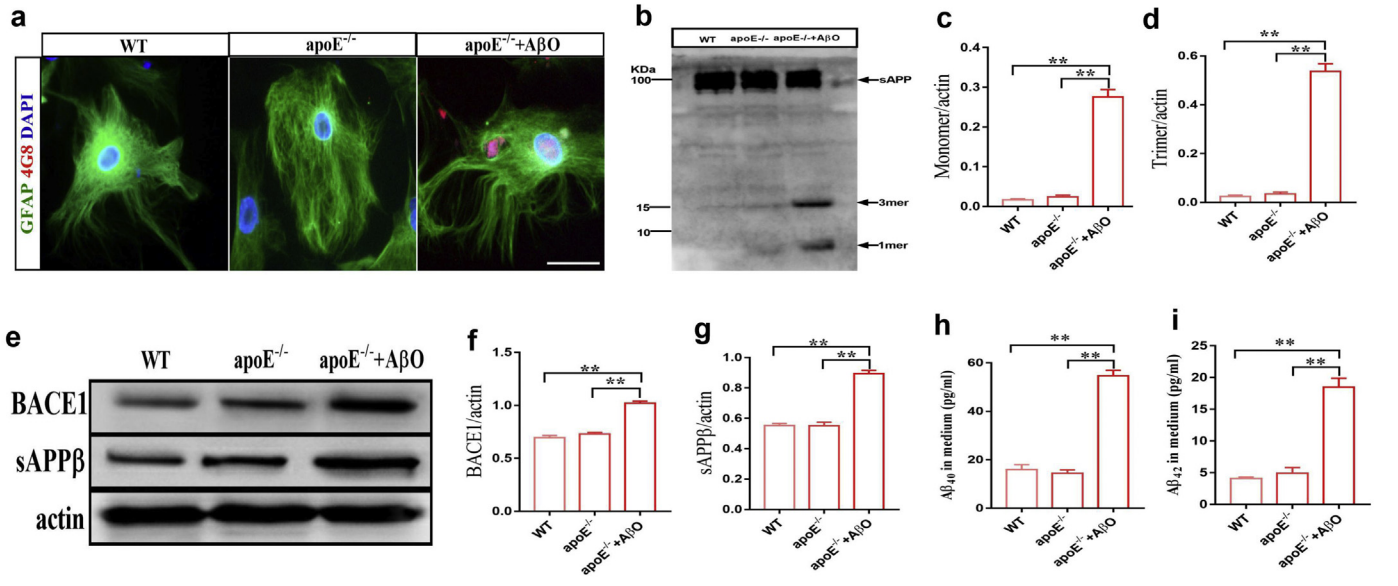

Fig. 7. ApoE is the key binding protein for Aβ assembly. (a) Representative images of primary WT and apoE$^{-/-}$astrocytes that were treated for 24 h with 5 μM AβOs; (b–d) Western blots and quantitative analysis of different Aβ assemblies (one-way ANOVA, c: $F = 176.8$, $p < .0001$; d: $F = 249.3$, $p < .0001$; n = 6/group); (e–g) Western blots and quantitative analysis of BACE1 and sAPPβ (one-way ANOVA, f: $F = 89.76$, $p < .0001$; g: $F = 92.29$, $p < .0001$; n = 6/group); (h and i) The levels of soluble Aβ40 and Aβ42 in the medium (one-way ANOVA, h: $F = 141.4$, $p < .0001$; i: $F = 70.08$, $p < .0001$; n = 6/group). The data are shown as the mean ± SEM, $^{*}p < .05$, $^{**}p < .01$; scale bar: 50 μm.

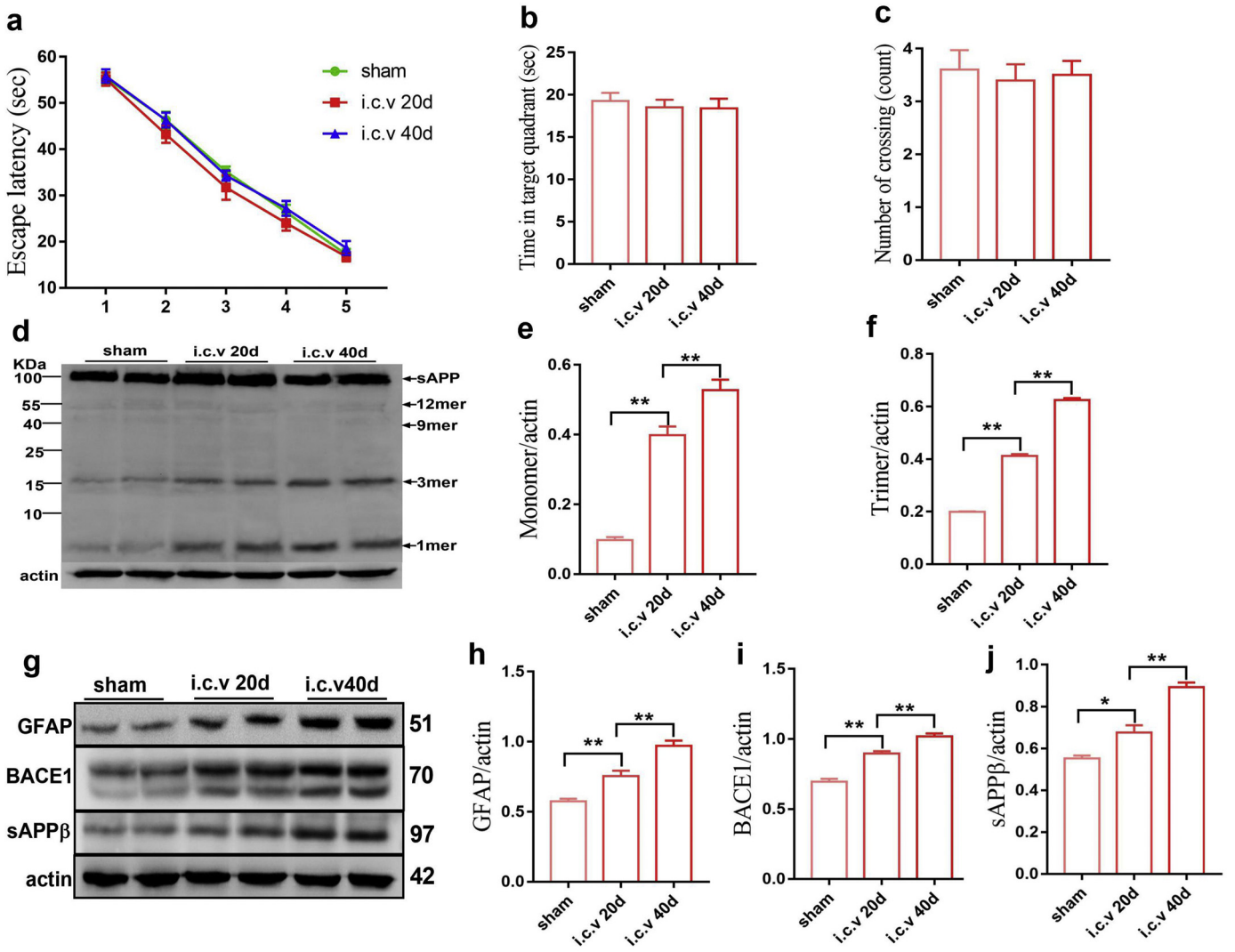

Fig. 8. I.c.v. injection of natural AβOs induced behavioral and biochemical changes in apoE$^{-/-}$ mice. (a) MWM escape latency during training (one-way ANOVA, F = 0.27, $p = .97$; $n = 8$/group). (b) Time in the target quadrant (one-way ANOVA, F = 0.21, $p = .81$; n = 8/group). (c) The number of crossings (one-way ANOVA, F = 0.099, $p = .91$; n = 8/group). (d) Western blot showing dynamic changes in Aβ assembly (4G8) in the brains of SD rats (time indicated above the lanes). The right lanes indicate the respective migration positions of monomers, trimers, nonamers, dodecamers and sAPP. (e, f) Bar graphs illustrating the quantitative analysis of monomers and trimers (one-way ANOVA,e: F = 88.47, p < .0001; f: F = 120.4, p < .0001; n = 6/group). (g) Western blots showing GFAP, BACE1 and sAPPβ in the mouse brain. (h-j) Bar graphs illustrating the quantitative analysis of Western blots (one-way ANOVA, h: F = 35.21, p < .0001; i: F = 74.73, p < .0001; j: F = 47.89, p < .0001; n = 6/group). The data are shown as the mean ± SEM (n = 6); *p < .05, **p < .01.

suppressed by pharmacological BACE1 inhibition. Hence, the natural AβOs did not induce obvious death in astrocytes but severely affected their normal functions, and BACE1 might therefore be a key therapeutic target.

A strong clue to the importance of Aβ oligomerization in AD pathogenesis came from the observation that the dysregulation between Aβ production and clearance caused Aβ to over-accumulate in the brain [35,36]. Redundant Aβ aggregates into various types of assemblies, including oligomers with different molecular masses, protofibrils and amyloid fibrils [37]. The mechanism underlying Aβ aggregation is also an unresolved issure. Several studies have clearly shown that apoE is essential for Aβ aggregation and deposition in APP transgenic AD mice [35,38–40]. ApoE is synthesized and secreted mainly by astrocytes in the CNS [41]. A previous study showed that apoE increased the level of AβOs in an isoform-dependent manner (apoE4 > apoE3 > apoE2); this effect appeared to be dependent on the apoE carboxy-terminal domain [42]. In our study, the AβOs activated astrocytes and induced the expression of apoE, which subsequently bound Aβ monomers to form AβOs. Natural AβOs can also induce the expression of BACE1 to produceredundant Aβ, but did not bind Aβ to form toxic AβOs (nonamer and dodecamer) in apoE$^{-/-}$ astrocytes and transgenic mice. These results support the notion that apoE was a key binding protein for the formation of toxic AβOs.

In the present study, the results showed that toxic AβOs were duplicated and amplified mainly in astrocytes, by inducing the expression of BACE1 and apoE. It has been demonstrated that Aβ accumulation triggers a neuroinflammatory state that plays a significant role in the progression of AD, and astrocytes are the key regulators of the neuroinflammation response [43]. Our results show that the natural AβOs induce reactive astrogliosis and increase inflammatory cytokines, which might be the main inducers of increases in the levels of BACE1 and apoE in astrocytes, but not neurons. However, the molecular mechanisms underlying these effects might be more complicated, and further work involving the use of multiple inhibitors or genetic knockdown approaches will be necessary to precisely dissect which signaling molecules are the most critical for the cytokine-stimulated elevations observed in BACE1 and apoE in astrocytes.

In conclusion, our results demonstrate that specific Aβ assemblies, nonamers and dodecamers, instigating cognitive deficits. These findings suggest the potential for developing precise diagnostic biomarkers to detect their correlates in humans with preclinical AD. We also reveal that toxic AβOs are produced and spread mainly in astrocytes by

inducing the overexpression of apoE, suggesting a novel mechanism underlying apoE function in progression of AD, and this opens a new perspective for searching for therapeutic targets for AD.

Ethics approval and consent to participate

All animal experiments were approved by the Ethics Committee of Capital Medical University (2010-X-098), and every effort was made to minimize the number and suffering of animals.

Availability data and materials

All relevant data are available from the authors upon reasonable request.

Declaration of interests

The authors declare that they have no conflicts of interest.

Authors' contributions

JP. J. and W. W. conceived the project, designed the experiments, and wrote the manuscript. W. W. and TT. H. performed animal experiments. TT. H. and QQ. W. performed primary cells experiments. W.W., and LFJ. performed data analyses. MN. Q. provided critical research reagents and critically read the manuscript. All authors read and approved the final manuscript.

Acknowledgments

This study was supported by the Key Project of the National Natural Science Foundation of China (81530036); the National Key Scientific Instrument and Equipment Development Project (31627803); Mission Program of Beijing Municipal Administration of Hospitals (SML20150801); Beijing Scholars Program, and Beijing Brain Initiative from Beijing Municipal Science & Technology Commission (Z161100000216137); CHINA-CANADA Joint Initiative on Alzheimer's Disease and Related Disorders (81261120571); Beijing Municipal Commission of Health and Family Planning (PXM2017_026283_000002). Funders had no roles in study design, data collection, data analysis, interpretation, and writing of the manuscript.

Appendix A. Supplementary data

Supplementary data to this article can be found online at https://doi.org/10.1016/j.ebiom.2019.03.049.

References

[1] Congdon EE, Sigurdsson EM. Tau-targeting therapies for Alzheimer disease. Nat Rev Neurol 2018;14(7):399–415.
[2] Hardy JA, Higgins GA. Alzheimer's disease: the amyloid cascade hypothesis. Science 1992;256(5054):184–5.
[3] Viola KL, Klein WL. Amyloid beta oligomers in Alzheimer's disease pathogenesis, treatment, and diagnosis. Acta Neuropathol 2015;129(2):183–206.
[4] Benilova I, Karran E, De Strooper B. The toxic Abeta oligomer and Alzheimer's disease: an emperor in need of clothes. Nat Neurosci 2012;15(3):349–57.
[5] Pagano K, Galante D, D'Arrigo C, Corsaro A, Nizzari M, Florio T, et al. Effects of Prion Protein on Aβ42 and Pyroglutamate-Modified AβpE3-42 Oligomerization and Toxicity. Mol Neurobiol 2019;56(3):1957–71.
[6] Hong W, Wang Z, Liu W, O'Malley TT, Jin M, Willem M, et al. Diffusible, highly bioactive oligomers represent a critical minority of soluble Abeta in Alzheimer's disease brain. Acta Neuropathol 2018;136(1):19–40.
[7] Matlack KE, Tardiff DF, Narayan P, Hamamichi S, Caldwell KA, Caldwell GA, et al. Clioquinol promotes the degradation of metal-dependent amyloid-beta (Abeta) oligomers to restore endocytosis and ameliorate Abeta toxicity. Proc Natl Acad Sci U S A 2014;111(11):4013–8.
[8] Lesne S, Koh MT, Kotilinek L, Kayed R, Glabe CG, Yang A, et al. A specific amyloid-beta protein assembly in the brain impairs memory. Nature 2006;440(7082):352–7.
[9] Birch AM. The contribution of astrocytes to Alzheimer's disease. Biochem Soc Trans 2014;42(5):1316–20.
[10] Prasad H, Rao R. Amyloid clearance defect in ApoE4 astrocytes is reversed by epigenetic correction of endosomal pH. Proc Natl Acad Sci U S A 2018;115(28) (E6640-E9).
[11] Liu CC, Zhao N, Fu Y, Wang N, Linares C, Tsai CW, et al. ApoE4 accelerates early seeding of amyloid pathology. Neuron 2017;96(5):1024–32 e3.
[12] Frost GR, Li YM. The role of astrocytes in amyloid production and Alzheimer's disease. Open Biol 2017;7(12).
[13] Armato U, Chiarini A, Chakravarthy B, Chioffi F, Pacchiana R, Colarusso E, et al. Calcium-sensing receptor antagonist (calcilytic) NPS 2143 specifically blocks the increased secretion of endogenous Abeta42 prompted by exogenous fibrillary or soluble Abeta25-35 in human cortical astrocytes and neurons-therapeutic relevance to Alzheimer's disease. Biochim Biophys Acta 2013;1832(10):1634–52.
[14] Osborn LM, Kamphuis W, Wadman WJ, Hol EM. Astrogliosis: an integral player in the pathogenesis of Alzheimer's disease. Prog Neurobiol 2016;144:121–41.
[15] Chiarini A, Armato U, Gardenal E, Gui L, Dal Pra I. Amyloid beta-exposed human astrocytes overproduce phospho-tau and overrelease it within exosomes, effects suppressed by calcilytic NPS 2143-further implications for Alzheimer's therapy. Front Neurosci 2017;11:217.
[16] Sofroniew MV, Vinters HV. Astrocytes: biology and pathology. Acta Neuropathol 2010;119(1):7–35.
[17] Freeman L, Guo H, David CN, Brickey WJ, Jha S, Ting JP. NLR members NLRC4 and NLRP3 mediate sterile inflammasome activation in microglia and astrocytes. J Exp Med 2017;214(5):1351–70.
[18] Zhang Y, Lu L, Jia J, Jia L, Geula C, Pei J, et al. A lifespan observation of a novel mouse model: in vivo evidence supports abeta oligomer hypothesis. PLoS One 2014;9(1):e85885.
[19] Wang Y, Cheng Z, Qin W, Jia J. Val97Leu mutant presenilin-1 induces tau hyperphosphorylation and spatial memory deficit in mice and the underlying mechanisms. J Neurochem 2012;121(1):135–45.
[20] Wang W, Lu L, Wu QQ, Jia JP. Brain amyloid-beta plays an initiating role in the pathophysiological process of the PS1V97L-Tg mouse model of Alzheimer's disease. J Alzheimers Dis 2016;52(3):1089–99.
[21] Jia J, Xu E, Shao Y, Jia J, Sun Y, Li D. One novel presenilin-1 gene mutation in a Chinese pedigree of familial Alzheimer's disease. J Alzheimers Dis 2005;7(2):119–24 [discussion 73-80].
[22] Escartin C, Bonvento G. Targeted activation of astrocytes: a potential neuroprotective strategy. Mol Neurobiol 2008;38(3):231–41.
[23] Khakh BS, Sofroniew MV. Diversity of astrocyte functions and phenotypes in neural circuits. Nat Neurosci 2015;18(7):942–52.
[24] Garai K, Verghese PB, Baban B, Holtzman DM, Frieden C. The binding of apolipoprotein E to oligomers and fibrils of amyloid-beta alters the kinetics of amyloid aggregation. Biochemistry 2014;53(40):6323–31.
[25] Zheng JY, Sun J, Ji CM, Shen L, Chen ZJ, Xie P, et al. Selective deletion of apolipoprotein E in astrocytes ameliorates the spatial learning and memory deficits in Alzheimer's disease (APP/PS1) mice by inhibiting TGF-beta/Smad2/STAT3 signaling. Neurobiol Aging 2017;54:112–32.
[26] Meyer-Luehmann M, Coomaraswamy J, Bolmont T, Kaeser S, Schaefer C, Kilger E, et al. Exogenous induction of cerebral beta-amyloidogenesis is governed by agent and host. Science 2006;313(5794):1781–4.
[27] Eisele YS, Obermuller U, Heilbronner G, Baumann F, Kaeser SA, Wolburg H, et al. Peripherally applied Abeta-containing inoculates induce cerebral beta-amyloidosis. Science 2010;330(6006):980–2.
[28] Hamaguchi T, Eisele YS, Varvel NH, Lamb BT, Walker LC, Jucker M. The presence of Abeta seeds, and not age per se, is critical to the initiation of Abeta deposition in the brain. Acta Neuropathol 2012;123(1):31–7.
[29] George S, Ronnback A, Gouras GK, Petit GH, Grueninger F, Winblad B, et al. Lesion of the subiculum reduces the spread of amyloid beta pathology to interconnected brain regions in a mouse model of Alzheimer's disease. Acta Neuropathol Commun 2014;2:17.
[30] Ostapchenko VG, Beraldo FH, Mohammad AH, Xie YF, Hirata PH, Magalhaes AC, et al. The prion protein ligand, stress-inducible phosphoprotein 1, regulates amyloid-beta oligomer toxicity. J Neurosci 2013;33(42):16552–64.
[31] Delekate A, Fuchtemeier M, Schumacher T, Ulbrich C, Foddis M, Petzold GC. Metabotropic P2Y1 receptor signalling mediates astrocytic hyperactivity in vivo in an Alzheimer's disease mouse model. Nat Commun 2014;5:5422.
[32] Pigoni M, Wanngren J, Kuhn PH, Munro KM, Gunnersen JM, Takeshima H, et al. Seizure protein 6 and its homolog seizure 6-like protein are physiological substrates of BACE1 in neurons. Mol Neurodegener 2016;11(1):67.
[33] Zacchetti D, Chieregatti E, Bettegazzi B, Mihailovich M, Sousa VL, Grohovaz F, et al. BACE1 expression and activity: relevance in Alzheimer's disease. Neurodegener Dis 2007;4(2–3):117–26.
[34] Leuba G, Wernli G, Vernay A, Kraftsik R, Mohajeri MH, Saini KD. Neuronal and nonneuronal quantitative BACE immunocytochemical expression in the entorhinohippocampal and frontal regions in Alzheimer's disease. Dement Geriatr Cogn Disord 2005;19(4):171–83.
[35] Ulrich JD, Ulland TK, Colonna M, Holtzman DM. Elucidating the role of TREM2 in Alzheimer's disease. Neuron 2017;94(2):237–48.
[36] Luo Q, Lin YX, Yang PP, Wang Y, Qi GB, Qiao ZY, et al. A self-destructive nanosweeper that captures and clears amyloid beta-peptides. Nat Commun 2018;9(1):1802.
[37] Kumar S, Henning-Knechtel A, Chehade I, Magzoub M, Hamilton AD. Foldamer-mediated structural rearrangement attenuates abeta oligomerization and cytotoxicity. J Am Chem Soc 2017;139(47):17098–108.
[38] Bien-Ly N, Gillespie AK, Walker D, Yoon SY, Huang Y. Reducing human apolipoprotein E levels attenuates age-dependent Abeta accumulation in mutant human amyloid precursor protein transgenic mice. J Neurosci 2012;32(14):4803–11.

[39] Bales KR, Verina T, Dodel RC, Du Y, Altstiel L, Bender M, et al. Lack of apolipoprotein E dramatically reduces amyloid beta-peptide deposition. Nat Genet 1997;17(3):263–4.
[40] Liao F, Yoon H, Kim J. Apolipoprotein E metabolism and functions in brain and its role in Alzheimer's disease. Curr Opin Lipidol 2017;28(1):60–7.
[41] Lin YT, Seo J, Gao F, Feldman HM, Wen HL, Penney J, et al. APOE4 causes widespread molecular and cellular alterations associated with Alzheimer's disease phenotypes in human iPSC-derived brain cell types. Neuron 2018;98(6):1294.
[42] Hashimoto T, Serrano-Pozo A, Hori Y, Adams KW, Takeda S, Banerji AO, et al. Apolipoprotein E, especially apolipoprotein E4, increases the oligomerization of amyloid beta peptide. J Neurosci 2012;32(43):15181–92.
[43] Gonzalez-Reyes RE, Nava-Mesa MO, Vargas-Sanchez K, Ariza-Salamanca D, Mora-Munoz L. Involvement of astrocytes in Alzheimer's disease from a neuroinflammatory and oxidative stress perspective. Front Mol Neurosci 2017;10:427.